NOVATEUR PUBLICATIONS
INTERNATIONAL JOURNAL OF INNOVATIONS IN ENGINEERING RESEARCH AND TECHNOLOGY
[IJIERT] ISSN: 2394-3696 Website: ijiert.org
VOLUME 11, ISSUE 02, February -2024

BLEACHING OF CRUDE PALM OIL BY ACTIVATED NISE CLAY: PROCESS KINETICS, ISOTHERM AND THERMODYNAMIC STUDIES

Nweke Chinenyenwa Nkeiruka,
Nwokedi Ikenna Chukwudi,
Chinyelu Charles Ebuka
Department of Chemical Engineering, Faculty of Engineering,
Nnamdi Azikiwe University, P.M.B. 5025, Awka, Anambra State, Nigeria.

Article History: *Received on: 05/12/2023* *Accepted on: 14/02/2024*

DOI: https://doi.org/10.26662/ijiert.v11i2.pp55-71

ABSTRACT

Alkaline-activated Nise clay was applied in the bleaching of crude palm oil as an adsorbent. The FTIR, SEM and XRF analyses were carried out on the raw and activated (ANIC) clay samples. The experimental process was carried out to determine the efficiency of ANIC in bleaching the crude palm oil. Adsorption kinetics and equilibrium isotherm studies were carried in other to understand and implement the adsorption process. The results obtained after analyses of the morphological properties, the elements and minerals present and the characteristic functional groups showed that the clay was kaolinite. The activation of the clay also brought about some changes in the morphological structure of the clay and also changed the functional groups. The efficiency of the bleaching process was observed to increase with increase in temperature. The optimum bleaching efficiency was 87.6% and was obtained at optimum conditions of 100 oC, 3.5 g and 50 mins. The kinetic adsorption studies indicated that the intra-particle diffusion model best described the bleaching process. The isotherm studies revealed that the Temkin isotherm model gave the best fitting using the experimental data because it gave the highest R^2 values of >0.98 at all the operating temperatures. The thermodynamic parameters indicated that the bleaching process became spontaneous between 353 and 373 K. The positive value of entropy (ΔS^0) obtained showed that the affinity of the adsorbent towards the adsorbate was high. The value of ΔH^0 was higher than 40 KJ.mol^{-1} indicating that the bleaching process was a chemisorption process.

Keywords: Crude palm oil, bleaching, alkaline activation, adsorption kinetics, equilibrium isotherm, thermodynamics

1.0 INTRODUCTION

The oil palm fruit is a very important agricultural produce in Nigeria (Ajemba et al., 2023; Nweke and Ajemba, 2022; Ojewumi et al., 2021; Nwabanne et al., 2018). The compression or solvent extraction of oil palm fruits leads to the production of crude palm oil (Bayram et al., 2021). They are refined with the use of either physical or chemical refining processes (Anyikwa et al., 2021; Bayram et al., 2021). The uses of crude palm oil cannot be overemphasized (Ajemba et al., 2023; Nweke et al., 2023; Nwabanne et al., 2018). However, crude palm oil contains impurities such as organic pigments which include carotenoids and chlorophyll, and other impurities like phosphates, sulphur, soaps and trace metal cations (Bayram et al., 2021). Carotenoids or beta-

carotene which are responsible for the red pigment in the palm oil influences the appearance, flavor and stability of prepared foods, hence the need for its removal (Permana et al., 2018; Nwabanne et al., 2018).

One of the refining techniques that can be applied to remove the unwanted beta-carotene include the bleaching process (Bayram et al., 2021; Permana et al., 2018). The effectiveness of the bleaching process can be effectively carried out by using adsorption method (Permana et al., 2018). Bleaching has the ability to concentrate specific substances preferentially from solutions unto the surfaces of the adsorbent. The importation of fuller's earth and activated carbon have been applied as adsorbents in developing countries such as Nigeria but the need to improve the use of locally-sourced adsorbents have led to the research for substitute materials (Nwabanne et al., 2018). The use of carbonaceous materials and clays such as bentonite, attapulgite and sepiolite have been applied in the bleaching of oils (Bayram et al., 2021).

In Nigeria, clay is a highly abundant material that can be used for bleaching (Ojewumi et al., 2021; Nwabanne et al., 2018). This is due to its high adsorptive capacity (Ajemba et al., 2023; Nwabanne et al., 2018; Salawudeen et al., 2014). Clay minerals vary in nature, even samples of clay from the same deposit differ in physical and chemical properties and in the type and amounts of impurities that are present in that type of clay (Abdullahi and Audi, 2017). Acid activation of clay has been used to enhance the adsorptive property of clay. It has been proven that bleaching efficiency increases with increase in acidity, porosity, pore-size distribution and specific surface area (Bayram et al., 2021; Nweke et al., 2023). But the use of acid-activated clay has a lot of disadvantages including soap formation during neutralization and the residual effect of the acid on the bleached palm oil (Salawudeen et al., 2014). The residual acid is reduced through washing the clay but the cost and time is a big challenge hence the need for an alternative. Nweke et al. (2023), Salawudeen et al. (2014) and Akinwande et al. (2014) investigated the suitability of alkaline-activated clays on the bleaching of oil. The authors discovered that alkaline activation had significant effect on the adsorptive power of the clay. The structure and morphology of the clay were also improved which aided adsorption process (Salawudeen et al., 2014).

It is very important to analyze the adsorption of beta-carotene onto clay to evaluate its bleaching properties. This can be studied with the use of kinetic models and is influenced by the properties of the adsorbent, adsorbent dosage, concentration of beta-carotene, temperature and contact time (Permana et al., 2018). Kinetics studies describe the rate of the removal of pollutant from the solution, rate of uptake of solute at the at the interface of the solid and solution, and aid in the design of the adsorption treatment plant (Nweke and Ajemba, 2022). A suitable kinetic model can be used to control the bleaching process as inappropriate kinetic model can lead to an inefficient bleaching process when applied to process control (Permana et al., 2018).

Different clays in Nigeria, have been studied in recent times for their bleaching abilities. However, these studies did not investigate the bleaching ability of the individual and combined effects of some activation parameters (temperature, contact time or adsorbent dosage) of alkali-activated Nise clay. Hence, the goal of this study was to evaluate the potentials of Nise clay in the bleaching of crude palm oil. The pseudo-first order kinetic model, the intra-particle diffusion model, the pseudo-second order kinetic model, and the Elovich equation were used to evaluate the kinetics of the bleaching process and to evaluate the kinetic studies of the process. Thermodynamic studies of the process were also studied.

2. MATERIALS AND METHODS

Collection of Materials

The clay used in this study was collected from Nise town (6.16168ºN, 7.0525ºE) in Awka South of Anambra state, Nigeria. The clay sample was dried under the sun for 24 hours. It was ground and sieved with a 150 μm

mesh size. The crude palm oil was collected from a palm oil processing plant in, Awka town, Anambra State. Other materials including distilled water, acetone and hydroxide (NaOH) and potassium hydroxide (KOH) were also collected and were of standard qualities.

Degumming of the oil

500 mL of crude palm oil was heated to 90 oC in a clean beaker. 0.25 ml of 85% phosphoric acid (H_3PO_4) was added and stirred for 10 minutes (Ifa et al., 2021). The oil was neutralized by adding 30 ml of 0.1 M sodium hydroxide (NaOH), stirred vigorously for 10 minutes before being filtered Mukasa-Tebandeke et al., 2016).

Characterizations of the clay sample

X-ray fluorescence analysis (XRF): The chemical compositions of the clay sample before and after alkaline-activation were carried out using X-Ray fluorescence analysis (X-supreme 8000) instrument (Abdullahi and Audu, 2017).

Fourier transform infrared spectroscopy analysis (FTIR): FTIR analysis was carried out using a Shimadzu FTIR-8400S spectrophotometer. All the FTIR spectra were recorded in the range of 4000 – 650 cm^{-1}. The analysis was carried out before and after alkaline-activation (Nweke et al., 2023; Abdullahi and Audu, 2017).

Scanning electron microscopy (SEM): Scanning electron microscope (SEM) (Phenom Proxy, PW 100-002, magnification-255x) was used to evaluate the surface morphology of the clay samples. The SEM analysis was carried out before and after alkaline-activation (Nweke and Ajemba, 2022; Abdullahi and Audu, 2017).

Alkaline Activation of the Clay Sample

500 ml of a mixture of 5 M potassium hydroxide (KOH) and 0.5 M of sodium hydroxide (NaOH) respectively was mixed with 150 g of the sieved raw Nise clay. The mixed slurry was heated for 2 hours at 100 oC. It was continuously stirred while the heating process took place. After the alkaline activation, the slurry was cooled at room temperature in the air. It was then filtered and the alkaline-activated Nise clay (ANIC) was washed with distilled water until the pH of the activated clay became neutral. The alkaline-activated clay (ANIC) was ground and sieved using a 150 μm mesh size after being dried at 105 oC for 24 hours in a memmert oven (Nweke et al., 2023; Salawudeen et al., 2014).

Experimental procedure

The degummed crude palm oil (100 ml) was put inside a 500 ml beaker and heated to the required temperature in a magnetic stirrer hot plate (model: SH85-2). One gram of ANIC was added to the beaker. The mixture was stirred continuously using a magnetic stirrer. It was heated at contact times of 10, 20, 30, 40, 45, and 50 mins. After the bleaching process, the mixture was filtered using a Whatman No. 1 filter paper and the absorbance of the bleached oil was tested using an ultra violet-visible spectrophotometer (model no - 752, P/N: C001). The absorbance of the bleached palm oil was determined at 550 nm wavelength for each oil sample obtained after bleaching at different process temperatures. The experiments were carried out at temperatures of 50, 70, 90, and 100 oC. The bleaching experiment was carried out as a batch process (Nweke et al., 2023).

Equilibrium adsorption studies

The experiment for equilibrium adsorption studies was carried out by varying the dosages of ANIC. This was done by repeating the bleaching experimental procedure with 1.0, 1.5, 2.0, 2.5, 3.0, and 7.0 g of ANIC. The bleaching procedure was carried out at the operating temperature of 100 oC and varying contact times of 10, 20, 30, 40, 45, and 50 mins. This was done to investigate the percentage decrease in absorbance of beta-carotene as the mass of clay increased (Nweke et al., 2023).

The bleaching Efficiency

The bleaching efficiency and the percentage color reduction were evaluated from the decrease in absorbance as shown in equation (1) (Abdullahi et al., 2022). Before the absorbance reading was taken, the samples were diluted with 10% (v/v) acetone (Nweke et al., 2023). The addition of acetone to unbleached palm oil was necessary in other to obtain the wavelength of the maximum absorbance (550 nm). This was applied in obtaining the absorbance of all the bleached palm oil samples, using acetone as reference (Abdullahi et al., 2022).

$$\text{Bleaching performance}\ (\%) = \frac{A_o - A_t}{A_o} \qquad (1)$$

Where A_o and At are the absorbances of the unbleached and bleached oil at time, t respectively.

Equilibrium isotherm modeling

Equilibrium adsorption isotherm describes the interactions between the adsorbate and the adsorbent at equilibrium at constant temperature. This aids in optimizing the application of adsorbents (Nweke et al., 2023, Gurubor and Chukwunonso, 2018). Information on adsorption equilibrium is necessary in other to understand, design and to implement the adsorption process (Silver et al., 2013). The adsorption isotherm study was carried out at four different temperatures (50, 70, 90 and 100 oC). The sorption equilibrium data from the experiments were fitted with the Langmuir, Freundlich, Temkin and Dubinin–Radushkevich, Jovanovic and Henry isotherm models as shown in Table 1.

Table 1. Equilibrium isotherm models fitted into the bleaching process using ANIC

Isotherm model	Isotherm equation	Reference
Langmuir	$\frac{X_e}{q_e} = \frac{1}{K_1 q_m} - \frac{X_e}{q_m}$ (2)	(Jasper et al., 2020)
Freundlich	$\log q_e = \log K + \frac{1}{n}\log X_e$ (3)	(Nnanwube et al., 2019)
Temkin	$q_e = B_1 \ln K_T + B_1 \ln X_e$ (4)	(Jasper et al., 2020)

Adsorption Kinetics Experiment

The adsorption kinetic analyzes the behaviour of adsorbates on adsorbents with the use of the effect of time on adsorption (Villabona-ortiz et al., 2022; Ebelegi et al., 2020). Kinetics study is beneficial in the decisions for the smooth running of the full-scale batch procedure (Anyikwa et al, 2021). The effect of contact time on the bleaching efficiency of crude palm oil using ANIC was studied with four kinetic models tabulated in Table 2. The pseudo-first-order, pseudo-second-order and Elovic models do not show the actual cause of adsorption but revealed the rate of the uptake of adsorbate by adsorption whereas the simulation of the intra-particle diffusion model was carried out to evaluate the mechanism controlling the adsorption process (Nweke et al., 2023; Ebelegi et al., 2020).

Table 2. Adsorption kinetic models fitted into the bleaching process using ANIC

Kinetic model	Kinetic equation		Reference
Pseudo-first-order	$\ln(q_e - q_t) = \ln q_e - k_1 t$	(10)	(Jasper et al., 2020)
Pseudo-second-order	$\frac{t}{q_t} = \frac{1}{k_2 q_e^2}\left(\frac{1}{q_e}\right)$	(11)	(Nweke et al., 2023)
Intra-particle	$q_t = k_d t^{0.5} + \varepsilon$	(12)	(Jasper et al., 2020)

Adsorption Thermodynamics

The thermodynamic parameters are evaluated from the experimental process easily because the bleaching process is temperature dependent. The evaluation of the feasibility and spontaneity of the process are very important in determining the thermodynamic properties (Ajemba et al., 2023). The thermodynamic properties include the Gibbs free energy (ΔG^o), change in enthalpy (ΔH^o), and change in entropy (ΔS^o). The Gibbs free energy of change evaluates the spontaneity of the process. The change in enthalpy (ΔH^o) at constant pressure is the energy supplied as heat when no extra work is done by the system. The enthalpy change evaluates the nature and mechanism of the adsorption process. The change in entropy (ΔS^o) showed the randomness at the solid/liquid interface. It also shows the structural changes of the adsorbent and adsorbate (Ebelegi et al., 2020). The Gibbs free energy is given as

$$\Delta G^o = RT\ln(k_d) \qquad (14)$$

Where, ΔG^o (J/mol) is the Gibb's free energy change, R is the universal gas constant (8.314 $Jmol^{-1}K^{-1}$), T is the absolute temperature (K) and k_d is the thermodynamic equilibrium constant.

$$k_d = \frac{q_e}{X_e} \qquad (15)$$

$$\ln k_d = \frac{\Delta S}{R} - \frac{\Delta H}{RT} \qquad (16)$$

$$\Delta G = \Delta H - T\Delta S \qquad (17)$$

The enthalpy and entropy values both in (J/mol) were evaluated using equation (16) where their values were calculated from the slope and intercept of the linear plot respectively from the plot of $k_d$against 1/T. The values of ΔG^o were estimated from Equation (17) (Nweke et al., 2023; Nweke and Ajemba., 2022).

3. RESULTS AND DISCUSSION

3.1 Result of Instrumental Analyses

Scanning electron microscopy (SEM), X-ray Fluorescence (XRF) analysis and Fourier transform infrared spectroscopy (FTIR) analysis were carried out on the raw and alkaline-activated clay samples as explained below.

Scanning electron microscopy (SEM)

SEM analyses show the morphology or texture, crystalline structure and surface topography of the bleaching adsorbent (Oli et al., 2017). Figure 1 and 2 showed the result of SEM analysis of the raw and alkaline-activated Nise clay samples respectively. The SEM analyses indicated that the clay samples were coarse and loosely packed having irregular and hexagonal edges with some well-formed flakes. This indicated that the clay samples were Kaolinites (Nweke et al., 2023; Oli et al., 2017). The coarseness of the particles indicated high silica and aluminium contents in the chemical composition of the clays (Jean Baptiste et al., 2020). The surface

areas and pores of ANIC became more developed after alkaline-activation (Nweke and Ajemba, 2022; Furquan et al., 2020).

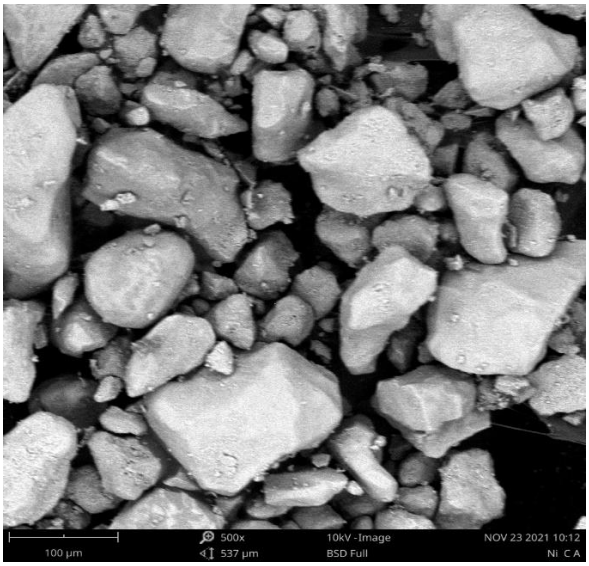

Fig. 1: SEM analysis of raw Nise clay @ 100 µm

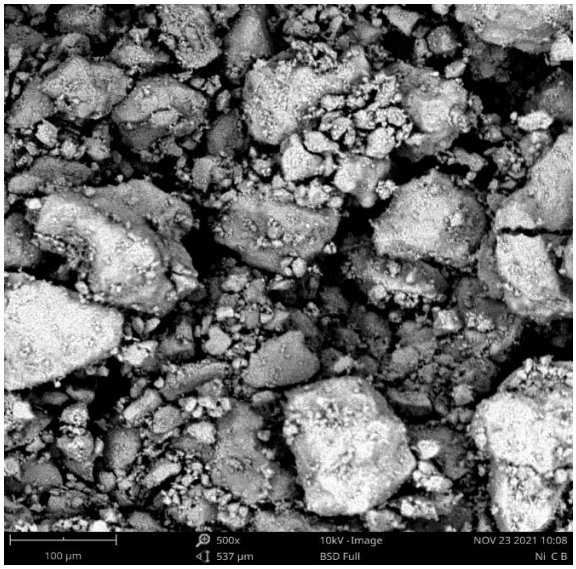

Fig. 2: SEM analysis of ANIC clay @ 100 µm

X-ray Fluorescence (XRF) analysis

It is important to carry out XRF analyses on the raw and activated clay samples to determine the chemical compositions of the minerals present in the clay (Oli et al., 2017). This is shown in Table 3. The composition of the elements in the raw and activated clay samples are seen in Table 4. The major oxides in the clay samples were silica oxide, ferrous oxide and alumina oxide. The result showed the presence of high silica oxide content on the raw (49.929%) and activated clay (61.010%) indicating that the clay can be used in the production of floor tiles due to its silica content (Oli et al., 2017). The ferrous oxide content was observed to reduce from 15.923% to 10.040%. The content of Aluminum oxide also reduced to 18.910% from 28.586%. There were traces of oxides such as nickel, calcium, zinc, and copper, etc. There was high increase in K_2O from 0.289% to 4.129% indicating an increase in the alkaline fluxes due to the alkaline activation (Nweke et al., 2023). The increase in silica content but a decrease in most of the components indicated that there was a partial destruction of the octahedral sheets by dissolution of exchangeable cations. This changed the structure of the clay structure thereby creating new pores and increased the surface area (Abdullahi et al., 2022).

Table 3: XRF result of oxides from raw and activated ANIC clays

Oxide	Concentration in raw Nise clay (%)	Concentration in ANIC (%)
SiO_2	49.929	61.010
V_2O_5	0.183	0.134
Cr_2O_5	0.019	0.039
MnO	0.199	0.137
Fe_2O_3	15.923	10.040
CO_3O_4	0.068	0.041
NiO	0.004	0.000
CuO	0.035	0.044
Nb_2O_3	0.021	0.025
MoO_3	0.003	0.000

WO_3	0.000	0.000
P_2O_5	0.046	0.000
SO_3	0.062	0.133
CaO	0.449	0.529
MgO	0.000	0.000
K_2O	0.289	4.129
BaO	0.006	0.000
Al_2O_3	28.586	18.910
Ta_2O_5	0.016	0.026
TiO_2	3.113	3.468
ZnO	0.012	0.006
Ag_2O	0.030	0.026
Cl	0.563	0.567
ZrO_2	0.414	0.711
SnO_2	0.000	0.000
PbO	0.025	0.014
Rb_2O	0.010	0.007
SrO	0.015	0.005

Table 4: XRF result of elements from raw and activated ANIC clays

Element	Concentration in raw Nise clay (%)	Concentration in ANIC (%)
O	46.594	47.053
Mg	0.000	0.000
Al	15.120	10.008
Si	23.339	28.519
P	0.020	0.000
S	0.025	0.053
Cl	0.563	0.567
K	0.240	3.427
Ca	0.321	0.378
Ti	1.866	2.079
V	0.102	0.075
Cr	0.013	0.027
Mn	0.154	0.106
Fe	11.137	7.023
Co	0.050	0.030
Ni	0.003	0.000
Cu	0.028	0.035
Zn	0.009	0.005
Rb	0.009	0.006
Sr	0.013	0.005
Zr	0.306	0.526
Nb	0.017	0.020
Mo	0.002	0.000
Ag	0.028	0.024
Sn	0.000	0.000
Ba	0.006	0.000
Ta	0.013	0.022
W	0.000	0.000
Pb	0.023	0.013

Fourier transform infrared spectroscopy (FTIR) analysis

Infrared spectroscopy (IR) is a widely used analytical technique to recognize the contents of clays (Jozanikohan and Abarghooei, 2022). (yet to add in reference).

The FTIR spectra of the raw Nise clay and ANIC samples are shown in Figs. 3 and 4 respectively. There were some modifications on the clay sample after alkaline activation when compared to the raw clay. This was due to the heat and chemical treatment given to the clay sample (Ajemba et al., 2023). The bands at 3697.5 cm^{-1}, 3652.8 cm^{-1}, 3623.0 cm^{-1} are assigned to OH stretching vibrations in the Si-OH and Al-OH groups of the tetrahedral and octahedral sheets of the raw clay and ANIC samples (Nweke et al., 2023). The wavelength in the range of 3697 cm^{-1} as obtained in the raw clay and ANIC samples showed that both clays were pure kaolinites ($Al_2(SiO_5)(OH)_4$) (Ajemba et al., 2023; Chen et al., 2015; Djomgoue et al., 2013). The wavenumbers of 1114.5 and 1032.5 cm^{-1} in both raw clay and ANIC samples respectively were assigned to Si-O stretching vibrations of kaolinite clay. The wavenumber of 909.5 cm^{-1} and 793.9 cm^{-1} seen in the raw clay indicated OH deformation which disappeared after alkaline-activation (Diko et al., 2016). The appearance of the wavenumber of 689.6 cm^{-1} in ANIC indicated the presence of Si-O quartz (Diko et al., 2016). The raw Nise clay and ANIC samples were concluded to be dominantly Kaolinite.

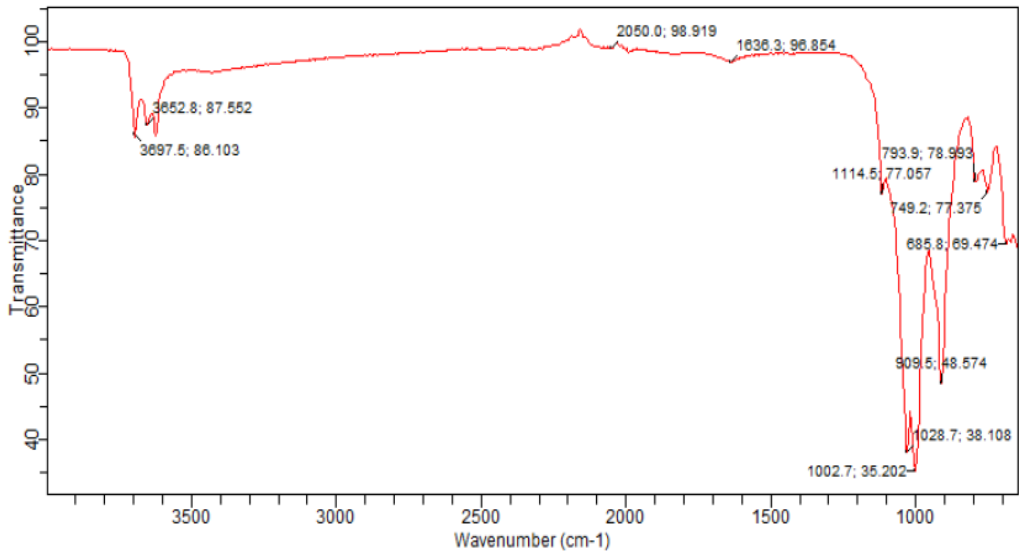

Fig. 3: FTIR analysis of raw Nise clay

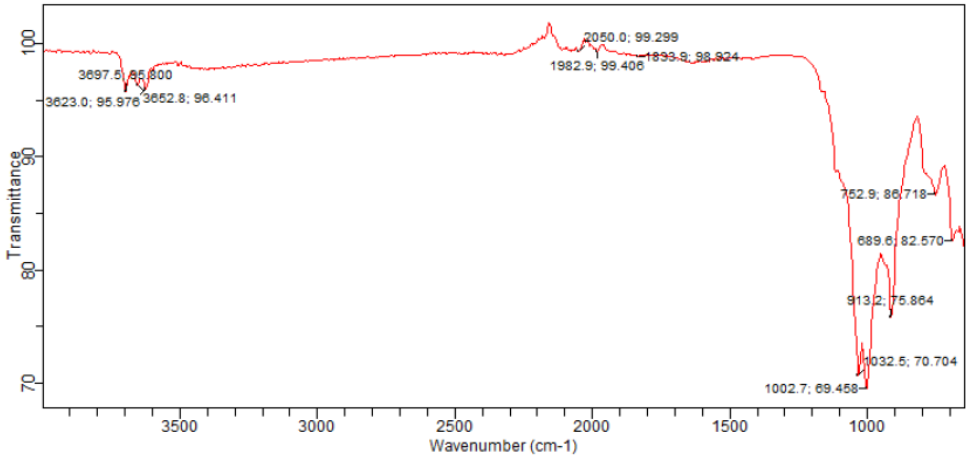

Fig. 4: FTIR analysis of alkaline-activated Nise clay (ANIC)

3.2 Effect of Process Parameters on the Bleaching Efficiency

The effects of contact time and temperature and adsorbent dosage were observed on the bleaching efficiency from the measurement of the absorbance values during bleaching experiment. The initial absorbance reading before the onset of the experiment was 2.5.

Effect of Contact time

It was observed that the absorbance decreased as the contact time increased as shown in Fig. 5. This result is similar to the result obtained by Anyikwa et al. (2021) and Yi et al. (2020). As seen in Tables 5 and 6 where the absorbances and bleaching efficiencies, the bleaching efficiency increases as the temperature and contact time increased. It was seen also that the bleaching efficiencies 50 mins contact time were 13.6% at 50 □C, 53.6% at 70 □C, 67.6% at 80 □C, 80.8% at 90 □C and 82.8% at 100 □C for 1 g of ANIC.

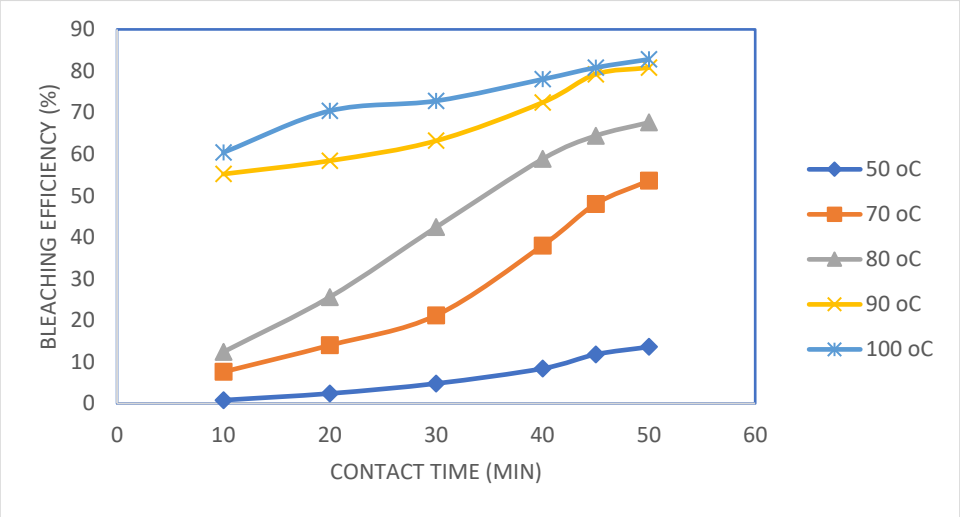

Fig. 5: Bleaching efficiencies of ANIC as a function of contact time at varying temperatures

Effect of Temperature

The effect of temperature was studied in the experimental process and the absorbance readings and bleaching efficiencies with temperature variation is shown in Tables 5 and 6 respectively. The plot of effect of temperature with bleaching efficiency is shown in Fig. 6. It was observed that bleaching efficiencies and adsorption increased with increasing temperature. This observation was also made by Asadu et al. (2021).

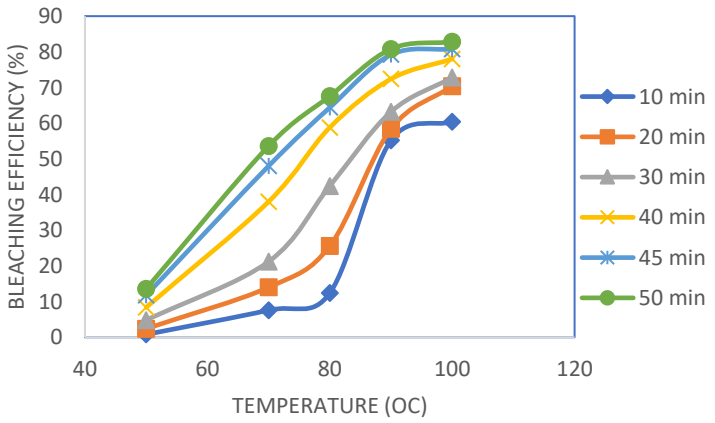

Fig. 6: Bleaching efficiencies of ANIC as a function of temperature at varying contact time

Table 5: Absorbance reading for ANIC from adsorption kinetics studies

Time (min)	Absorbance				
	50 ºC	70 ºC	80 ºC	90 ºC	100 ºC
10	2.48	2.31	2.19	1.12	0.99
20	2.44	2.15	1.86	1.04	0.74
30	2.38	1.97	1.44	0.92	0.68
40	2.29	1.55	1.03	0.69	0.55
45	2.21	1.30	0.89	0.52	0.48
50	2.16	1.16	0.81	0.48	0.43

Table 6: Bleaching performance for ANIC from adsorption kinetics studies

Time (min)	Bleaching Performance (%)				
	50 ºC	70 ºC	80 ºC	90 ºC	100 ºC
10	0.8	7.6	12.4	55.2	60.4
20	2.4	14.0	25.6	58.4	70.4
30	4.8	21.2	42.4	63.2	72.8
40	8.4	38.0	58.8	72.4	78.0
45	11.8	48.0	64.4	79.2	80.8
50	13.6	53.6	67.6	80.8	82.8

Effect of Adsorbent Dosage

The effect of adsorbent dosage is shown in Fig. 7. The absorbance values and percentage removal efficiencies with effect of adsorbent dosage is seen in Tables 7 and 8 respectively. The number of active sites available for adsorption is directly influenced by the adsorbent dosage, hence the efficiency of the process (Villabonna-ortiz et al., 2022). The result showed that increase in ANIC dosage increased the amount of beta carotene adsorbed from the crude palm oil. This is because the increase in adsorbent dosage increased the number of active sites of the activated carbon available to the beta carotene for adsorption. This increased the rate of adsorption (Gurunubor and Chukwunonso, 2018).

When the adsorbent dosage was increased to 3.5 g, there was competition between solute ions for the available binding sites, overlapping or aggregation of adsorption sites and low surface area, thereby reducing the contact of the solute ion on the adsorbent (Villabonna-ortiz et al., 2022). The data obtained indicated that the bleaching efficiency increased with increase in dosage up to an optimum dosage of 3.0 g. Beyond 3.0 g, increase in the activated clay did not cause a decrease in absorbance nor the bleaching efficiency.

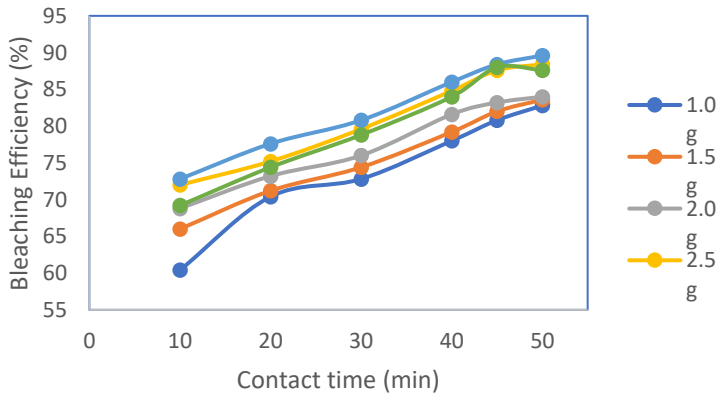

Fig. 7: Bleaching efficiencies of ANIC as a function of adsorbent dosage at varying contact time

Time (min)	Absorbance					
	1.0 g	1.5 g	2.0 g	2.5 g	3.0 g	3.5 g
10	0.99	0.85	0.78	0.70	0.68	0.77
20	0.74	0.72	0.67	0.62	0.56	0.64
30	0.68	0.64	0.60	0.51	0.48	0.53
40	0.55	0.52	0.46	0.38	0.35	0.40
45	0.48	0.45	0.42	0.31	0.29	0.30
50	0.43	0.41	0.40	0.29	0.26	0.31

Table 8: Bleaching Performance for ANIC clay equilibrium adsorption studies at 100 oC

Time (min)	Bleaching Performance (%)					
	1.0 g	1.5 g	2.0 g	2.5 g	3.0 g	3.5 g
10	60.4	66.0	68.8	72.0	72.8	69.2
20	70.4	71.2	73.2	75.2	77.6	74.4
30	72.8	74.4	76.0	79.6	80.8	78.8
40	78.0	79.2	81.6	84.8	86.0	84.0
45	80.8	82.0	83.2	87.6	88.4	88.0
50	82.8	83.6	84.0	88.4	89.6	87.6

Adsorption Kinetic Modelling

The adsorption kinetics of beta-carotene in palm oil onto ANIC can be described by kinetic models. Kinetic modelling of the adsorption of beta-carotene is used for the analysis of the performance of the experimental process (Permana et al., 2018). Kinetics study is used to analyze the mechanism of adsorption and the controlling steps which enables the smooth running of a full-scale batch procedure (Villabonna-ortiz et al., 2022; Anyikwa et al., 2021). In this study, the pseudo-first-order, pseudo-second-order, and intra-particle diffusion models were studied. The pseudo-first-order model is mainly used in the analysis of adsorption of adsorbates from aqueous solutions. The model describes the adsorption rates and is proportional to number of unoccupied binding sites on the adsorbent. The plot of Pseudo-first-order can be seen in Fig 8. It can be seen that the pseudo-first-order model satisfactorily fitted the kinetics of beta-carotene on ANIC, according to the R^2 of >0.85 with the highest R^2 value of 0.9724 at 80 oC.

The pseudo-second-order kinetic model is used to describe the adsorption of adsorbates onto adsorbents where the chemical bonding between the functional groups on the adsorbent surface and the adsorbates determine the adsorption capacity of adsorbent. This model predicts the order of the adsorption process (Ebelegi et al., 2020). The plot of Pseudo-second-order can be seen in Fig. 9. Only the data obtained at 50, 90 and 100 oC fitted the kinetics study using the pseudo-second-order model, according to the R^2 of >0.85 with the highest R^2 value of 0.996 at 100 oC.

The results showed that the experimental data most fitted the pseudo-second-order kinetic model when compared to other models since it has the most linear fit with a regression coefficient, R^2 of 0.996. Anyikwa et al. (2021) also reported that the pseudo-second-order gave a better fit than other models. The high regression coefficient of the pseudo-second order model showed that the adsorption of beta-carotene onto ANIC followed the chemisorption mechanism which was the rate controlling step in the adsorption process (Nwobasi et al., 2020; Permana et al., 2018; Gurunubor and Chukwunonso, 2018).

For the intra-particle diffusion model plot, the linear graph passing through the origin indicates that the intra-particle diffusion alone is the rate determining step. However, when an intercept ‘C’ is obtained from the plot

indicates that film diffusion also takes place simultaneously with the value of the intercept hinting on the thickness of the boundary layer (Ebelegi et al., 2020).

Fig. 10 presents the plot of the intra-particle diffusion at all temperatures. The intra-particle diffusion model showed higher correlations to the experimental data than the other models. Hence, it is the model that best described the bleaching process. The linear plot of qt versus $t^{1/2}$ did not pass through the origin for all temperatures, hence the intra-particle diffusion is not the sole rate-limiting process. This was due to the difference in mass transfer rate from the initial to the final stage of adsorption (Nwabanne et al., 2018). Table 9 presents the kinetic parameters for the pseudo-first-order, the pseudo-second-order and the intra-particle diffusion models at all temperatures.

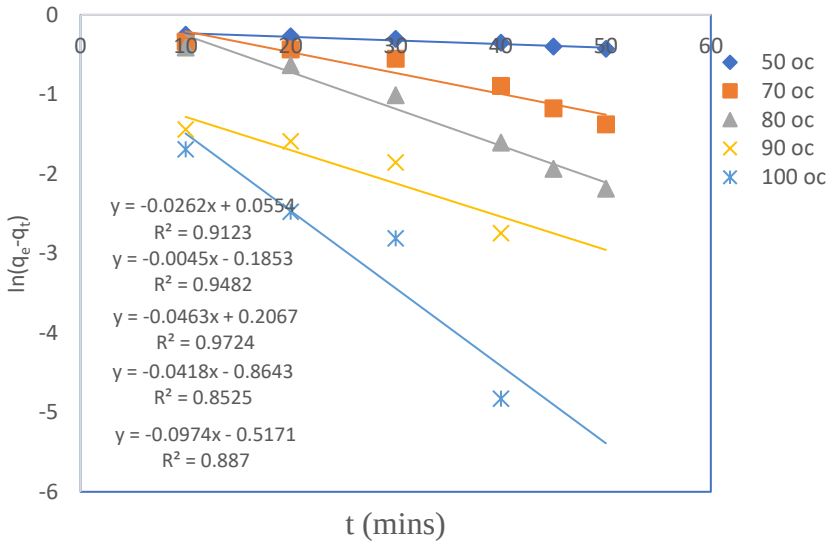

Fig. 8: Plot of pseudo-first-order kinetic

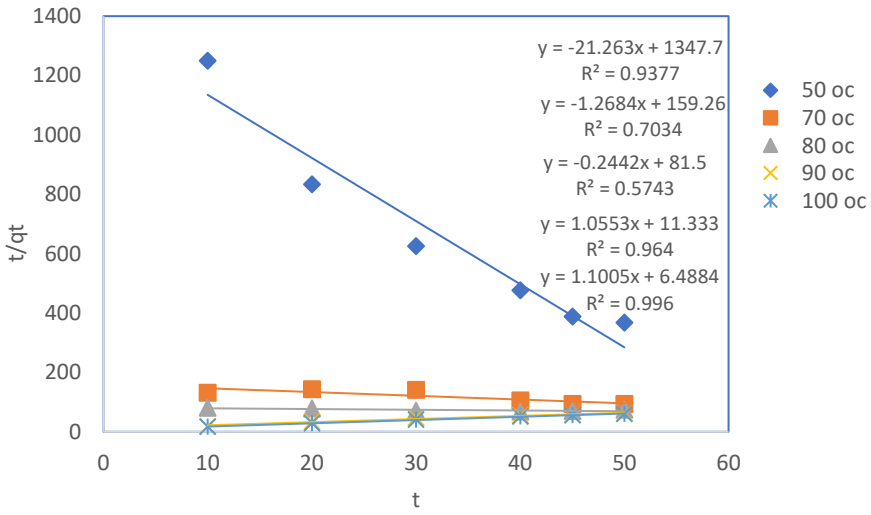

Fig. 9: Plot of pseudo-second-order kinetic model

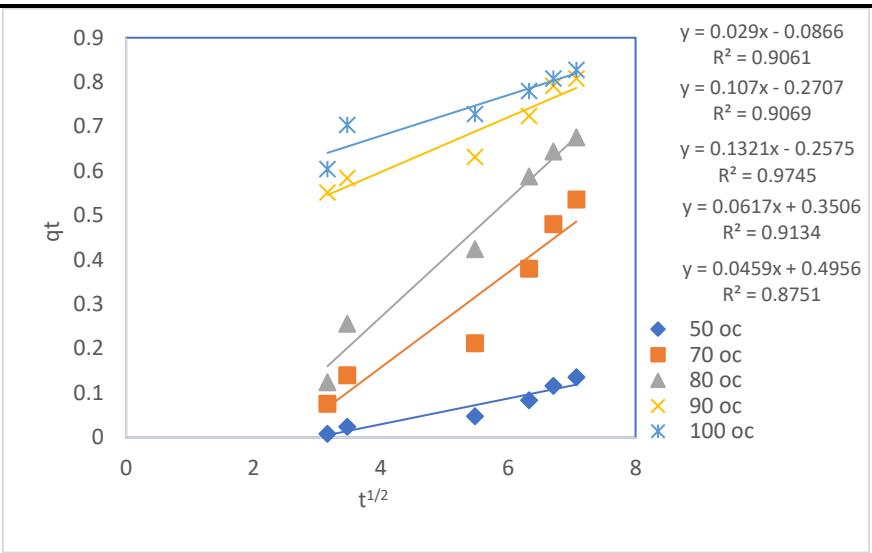

Fig. 10: Plot of intra-particle diffusion model

Table 9. Parameters from Adsorption Kinetics study for the bleaching of palm oil usingANIC

Kinetic model	Kinetic constants	Temperature (oC)				
		50	70	80	90	100
Pseudo-first-order	K_1 (min^{-1})	0.0262	0.0045	0.0463	0.0418	0.0974
	q_e (mg/g)	1.0570	0.8309	1.2296	0.4213	0.5962
	R^2	0.9123	0.9482	0.9724	0.8525	0.8870
Pseudo-second-order	K_2 (g/mg min)	-0.0158	-0.0080	-0.0030	0.0931	0.1696
	q_e (mg/g)	-0.0470	-0.7884	-4.0950	0.9476	0.9087
	R^2	0.9377	0.7034	0.5743	0.9640	0.9960
Intra-particle diffusion	K_d	0.0290	0.1070	0.1321	0.0617	0.0459
	ε	-0.0866	-0.2707	-0.2575	0.3506	0.4956
	R^2	0.9061	0.9069	0.9745	0.9134	0.8751

Adsorption isotherm modeling

The adsorption isotherm is an important requirement for the design of an adsorption system because it shows the relationship between the amount adsorbed from the liquid phase by the adsorbent and its concentration at constant temperature (Asadu et al., 2021). The parameters for isotherms were determined by linear fitting. The isotherm parameters calculated from the isotherm plots with their regression coefficients are listed in Table 10.

The rate of adsorption, K_1 in the Langmuir model presented a positive correlation with temperature unlike in Almeida et al. (2019) where the opposite was the case. The positive correlation indicated that the affinity between the adsorbate and adsorbent increased with increase in temperature. The adsorption capacity represented by the parameters q_m and K in Langmuir and Freundlich isotherms respectively increased with temperature indicating an endothermic adsorption process. The parameter n in the Freundlich model didn't show a positive correlation with temperature. This indicated a low adsorption intensity (Almeida et al., 2019). The results for the four adsorption isotherms indicate that the Temkin isotherm model gave the best fitting for

the adsorption data because the model displayed the highest R^2 values. Okafor et al. (2019) also reported that the Temkin model gave the best fit for the adsorption data.

Table 10. Adsorption isotherm parameters for the bleaching of palm oil using ANIC

Adsorption isotherm model	Kinetic constants	Temperature (oC)				
		50	70	80	90	100
Langmuir	K_1 (l/mg)	-0.8794	-0.4855	-0.3380	-0.1588	-0.0757
	q_m (mg/g)	0.0017	0.1016	0.2853	4.9116	6.6401
	R^2	0.589	0.7714	0.8272	0.9919	0.9906
Freundlich	K (l/g)	5.26×10^{-19}	0.0025	0.0283	0.3627	0.4257
	n	-0.5265	-0.9480	-1.1605	-2.5	-2.8035
	R^2	0.8693	0.9051	0.8971	0.9802	0.9695
Temkin	K_T (mg/g)	0.9983	0.9408	0.8564	0.3394	0.2469
	b (KJ/mol)	-2.8982	-4.2741	-5.3634	-10.0835	-11.6759
	R^2	0.9997	0.9934	0.9857	0.9906	0.9839

Adsorption Thermodynamics

The values evaluated from the thermodynamic studies are shown in Table 11. Gibbs free energy of change is used to evaluate the spontaneity and feasibility of adsorption processes. A negative ΔG^0 value validates a spontaneous process while a positive ΔG^0 value indicates that a non-spontaneous process took place (Ebelegi et al., 2020). It can be observed from Table 11 that spontaneity was observed between 353 and 373 K. The positive value of entropy (ΔS^0) obtained showed that the affinity of the adsorbent towards the adsorbate was high. It also indicated that there was an increase in the randomness at the solid/liquid interface (Ebelegi et al., 2020). This also showed that the process was feasible and did not violate the second law of thermodynamics (Thompson et al., 2020). The adsorption of carotene from crude palm oil using ANIC was observed to be endothermic. Thompson et al. (2020) reported on some research processes that were endothermic. Nweke et al. (2023) also reported that the bleaching of crude palm oil was endothermic. The value of ΔH^0 was higher than 40 $KJ.mol^{-1}$ indicating that the bleaching process was a chemisorption process (Nweke et al., 2023).

Table 11. Thermodynamic Parameters from the bleaching of palm oil using ANIC at 50 min

Temperature (K)	Thermodynamic Properties			
	ΔG^o (J/mol)	ΔH^o (J/mol)	ΔS^o (J/mol)	R^2
323	4,393.13			
343	281.33			
353	-1,774.57			
363	-3,830.47			
373	-5,886.37	70,798.70	205.59	0.9668

CONCLUSION

Some known quantity of local Nise clay was collected and alkaline activation using a mixture of 5 M potassium hydroxide (KOH) and 0.5 M of sodium hydroxide (NaOH) was carried out on the clay. The FTIR, SEM and XRF analyses were carried out on the raw and activated (ANIC) clay samples. The results obtained after analyses of the morphological properties, the elements and minerals present and the characteristic

functional groups showed that the clay was kaolinite. The activation of the clay also brought about some changes in the morphological structure of the clay and also changed the functional groups. Increase in temperature during the bleaching process improved the bleaching performance. The optimum conditions for the process efficiency was obtained at 100 oC, 3.5 g and 50 mins. This resulted in the bleaching efficiency of 87.6%. The kinetic adsorption studies indicated that the intra-particle diffusion model best described the bleaching process. The isotherm studies revealed that the Temkin isotherm model gave the best fitting using the experimental data because it gave the highest R^2 values of >0.98 at all the operating temperatures. The thermodynamic parameters indicated that the bleaching process became spontaneous between 353 and 373 K. The positive value of entropy (ΔS^0) obtained showed that the affinity of the adsorbent towards the adsorbate was high. The value of ΔH^0 was higher than 40 $KJ.mol^{-1}$ indicating that the bleaching process was a chemisorption process. From these conclusions, ANIC can be applied as a potential adsorbent for the bleaching of crude palm oil.

REFERENCES

1. Abdullahi, S.L and Audu, A.A. (2017) Comparative analysis on chemical composition of bentonite clays obtained from Ashaka and Tango Deposits in Gombe State, Nigeria. ChemSearch Journal, 8(2): 35 – 40.
2. Abdullahi, Y.A., Langkuk, M.T., Joseph, K.O. Adole, V.O., Segun, A.A. Mohammed, S.U. and Dawes, E.M. (2022) Preparation, Characterization and Comparison of adsorbents from Kirfi kaolin clay with Commercial bleaching Clay. International Journal of Research and Scientific Innovation (IJRSI), IX(VII): 116-120.
3. Ajemba, R.O., Nweke C.N., Okoye C.C. and Nwachukwu J.O. (2023) Adsorption of carotene from crude palm oil by Activated Achalla clay. Journal of Engineering Research and Reports, 24(5): 1-17. DOI: 10.9734/JERR/2023/v24i5813.
4. Akinwande B.A., Salawudeen T.O., Arinkoola A.O. and Jimoh M.O. (2014) A suitability assessment of alkali activated clay for application in vegetable oil refining. International Journal of Engineering and Advanced Technology Studies, 2(1): 1-12.
5. Almeida, E.S., Carvalho, A.C.B., Soares, I.O., Valadares, L.F., Mendonça, A.R.V., José Silva Jr, I. and Monteiro S. (2019) Elucidating how two different types of bleaching earths widely used in vegetable oils industry remove carotenes from palm oil: Equilibrium, kinetics and thermodynamic parameters. Food Research International 121 (2019) 785- 797.
6. Anyikwa, S.O., Nwakaudu, M.S., Nzeoma, C. and Yakubu, E. (2021) Kinetics and equilibrium studies of colour pigments removal from crude palm oil using acid activated kaolin clay and mathematical method. International Journal of Science and Engineering Investigations, 10(116): 30-44.
7. Asadu, C.O., Ezema, C.A., Onu, C.E., Ike, I.S., Ohiomor, E.O. and Umeagukwu, E.O. (2021) Development of an adsorbent for the remediation of crude oil polluted water using stearic acid grafted coconut husk (Cocos nucifera) composite. Applied Surface Science Advances 6 (2021) 100179.
8. Bayram, H., Ustunisik, G., Önal, M. and Sarıkaya, Y. (2021) Optimization of bleaching power by sulfuric acid activation of bentonite. Clay Minerals. 56:148-155. doi:10.1180/clm.2021.28.
9. Chen Y, Zou C, Mastalerz M, Hu S, Gasaway C. and Tao, X. (2015) Applications of micro-fourier transform infrared spectroscopy (FTIR) in the geological sciences - A review. Int J Mol Sci., 16:30223–30250.

10. Diko, M., Ekosse G. and Ogola, J. (2016) Fourier Transform Infrared Spectroscopy and Thermal Analyses of Kaolinitic Clays from South Africa and Cameroon. Acta Geodyn. Geomater., 13(2), xx1–x10. DOI: 10.13168/AGG.2015.0052.
11. Djomgoue, P. and Njopwouo, D. (2013) FT-IR spectroscopy applied for surface clays characterization. J Surf Eng Mat Adv Technol., 3:275-282. DOI:http://dx.doi.org/10.4236/jsemat.2013.34037.
12. Ebelegi, A.N., Ayawei, N. and Wankasi, D. (2020) Interpretation of adsorption thermodynamics and kinetics. Open Journal of Physical Chemistry, 2020, 10, 166-182.
13. Furquan, B., Murtuza, A.S. and Feroz, S. (2018) Palm oil bleaching using activated carbon prepared from Neem leaves and waste tea. Int J Eng Res Technol., 13(4):620-624.
14. Golnaz Jozanikohan and Mohsen Nosrati Abarghooei (2021) The Fourier transform infrared spectroscopy (FTIR) analysis for the clay mineralogy studies in a clastic reservoir. Journal of Petroleum Exploration and Production Technology. https://doi.org/10.1007/s13202-021-01449-y.
15. Gunorubor, A.J. and Chukwunonso, N. (2018) Kinetics, equilibrium and thermodynamics studies of Fe^{3+} ion removal from aqueous solutions using periwinkle shell activated carbon. Advances in Chemical Engineering and Science, 8: 49-66.
16. Ifa, L., Wiyani, L., Nurdjannah. N., Ghalib, A.M.T., Ramadhaniar, S., Kusuma, H.S. (2021) Analysis of bentonite performance on the quality of refined crude palm oil's color, free fatty acid and carotene: the effect of bentonite concentration and contact time. Heliyon, 7 (2021) e07230.
17. Jasper, E.E., Ajibola, V.O., Onwuka, J.C. (2020) Nonlinear regression analysis of the sorption of crystal violet and methylene blue from aqueous solutions onto an agro-waste derived activated carbon. Applied Water Science, 10(132): 1-11.
18. Jean Baptiste, B.M., Daniele, B.K., Eko, M.C., Tekoumbo, T.L.C., Elimbi, A. and Kamga, R. (2020) Adsorption mechanisms of pigments and free fatty acids in the discoloration of shea butter and palm oil by an acid-activated Cameroonian smectite. Sci Afr., 9(2020) e00498.
19. Mukasa-Tebandeke I.Z., Wasajja-Tebandeke, H., Schumann, A. and Lugolobi, F. (2016) Bleaching Edible Oils Using Clay from Kangole, Moroto District, North Eastern Uganda. Journal of Analytical & Bioanalytical Techniques, 7(3): 1000320.
20. Nnanwube, I.A., Onukwuli, O.D., Okafor, V.N., Obibuenyi, J.I., Ajemba, R.O., Chukwuka, C.C. (2019) Equilibrium, kinetics and optimization studies on the bleaching of palm oil using activated Karaworokaolinite. J. Mater. Environ. Sci., 11(10): 1599-1615.
21. Nwabanne, J.T., Onu, C.E., Nwankwoukwu, O.C. (2018) Equilibrium, kinetics and thermodynamics of the bleaching of palm oil using activated Nando clay. J Eng Res Rep.,1(3):1-13.
22. Nweke, C.N and Ajemba R.O. (2022) Clay characterization and bleaching of crude palm oil using acid-activated Nibo clay. Bioremediation Science and Technology Research, 10(1): 14-21.
23. Nweke, C.N., Onu, C.E. and Iheanacho C.O. (2023) Kinetic and thermodynamic studies of crude palm oil bleaching using Amansea Clay. Asian Journal of Applied Chemistry Research, 13(1): 23-32.
24. Nwobasi, V.N., Igbokwe, P.K., Onu, C.E. (2020) Removal of methylene blue dye from aqueous solution using modified Ngbo clay. Journal of Materials Science Research and Reviews, 5(2): 33-46.
25. Ojewumi, M.E., Ehinmowo, A.B., Obanla, O.R., Durodola, B.M., Ezeocha, R.C. (2021) Comparative analysis on the bleaching of crude palm oil using activated groundnut hull, snail shell and rice husk. Heliyon, 7 (2021) e07747. https://doi.org/10.1016/j.heliyon.2021.e07747.

26. Okafor, V.N., Nnanwube, I.A., Obibuenyi, J.I., Onukwuli, O.D. and Ajemba, R.O. (2019) Removal of pigments from palm oil using activated Ibusa kaolinite: Equilibrium, kinetic and thermodynamic studies. Journal of Minerals and Materials Characterization and Engineering, 2019, 7, 157-170.

27. Oli, S.C., Kamalu, C.I.O., Obijiaku, J.C., Opebiyi, S.O., Oghome, P. and Nkwocha, A.C. (2017) A study on the bleaching properties of locally sourced clay (Ukpor clay) for the processing of palm oil. International Journal of Modern Research in Engineering and Technology (IJMRET), 2(5):4-29.
28. Permana, T., Noor, E. and Arkeman, Y. (2018) Evaluation of Kinetic Models of Beta-Carotene Adsorption from Palm Oil onto Bentonite. International Journal of Scientific & Technology Research, 7(4):23- 31.
29. Salawudeen, T.O., Arinkoola, A.O., Jimoh, M.O., Akinwande, B.A. (2014) Clay characterization and optimisation of bleaching parameters for palm kernel oil using alkaline activated clays. Journal of Minerals and Materials Characterization and Engineering. 2014; 2:586-597.
30. Silva, S.M., Sampaio, K.A., Ceriani, R., Roland Verhé, R., Stevens, C., De Greyt, W., Meirelles, A.J.A. (2013) Adsorption of carotenes and phosphorus from palm oil onto acid activated bleaching earth: Equilibrium, kinetics and thermodynamics. Journal of Food Engineering, 118: 341–349.
31. Thompson, C.O., Ndukwe, A.O. and Asadu, C.O. (2020) Application of activated biomass waste as an adsorbent for the removal of lead (II) ion from wastewater. Emerging Contaminants. 6(2020): 259- 267.
32. Villabona-Ortíz, A., Figueroa-Lopez, K.J. and Ortega-Toro, R. (2022) Kinetics and adsorption equilibrium in the removal of Azo-Anionic dyes by modified cellulose. Sustainability, 14(3640): 1-19. https://doi.org/10.3390/su14063640.
33. Yi, Y.M., Myat, K.T., Soe, S.N., Kyaw, N. (2020) Removal of colouring materials and impurities in palm oil by using bentonite clay. J. Myanmar Acad. Arts Sci., 2020(XVIII):1A.